

Adsorption of CO_2 on MgAl layered double hydroxides: Effect of intercalated anion and alkaline etching time

Yan-Yan Feng(冯艳艳), Xiao-Di Niu(牛潇迪), Yong-Hui Xu (徐永辉), and Wen Yang(杨文)
Citation: Chin. Phys. B, 2021, 30 (**4**): 048101. DOI: 10.1088/1674-1056/abd750
Journal homepage: http://cpb.iphy.ac.cn; http://iopscience.iop.org/cpb

What follows is a list of articles you may be interested in

Influence of an inserted bar on the flow regimes in the hopper

Yi Peng(彭毅), Sheng Zhang(张晟), Mengke Wang(王梦柯), Guanghui Yang(杨光辉), Jiangfeng Wan(万江锋), Liangwen Chen(陈良文), and Lei Yang(杨磊)
Chin. Phys. B, 2021, 30 (**2**): 028101. DOI: 10.1088/1674-1056/abcf40

Morphological modifications of C_{60} crystal rods under hydrothermal conditions

Ming-Run Du(杜明润), Shi-Xin Liu(刘士鑫), Jia-Jun Dong(董家君), Ze-Peng Li(李泽朋), Ming-Chao Wang (王明超), Tong Wei(魏通), Qing-Jun Zhou(周青军), Xiong Yang(杨雄), and Peng-fei Shen(申鹏飞)
Chin. Phys. B, 2020, 29 (**12**): 128102. DOI: 10.1088/1674-1056/abc0d8

A numerical study of dynamics in thin hopper flow and granular jet

Meng-Ke Wang(王梦柯), Guang-Hui Yang(杨光辉), Sheng Zhang(张晟), Han-Jie Cai(蔡汉杰), Ping Lin(林平), Liang-Wen Chen(陈良文), Lei Yang(杨磊)
Chin. Phys. B, 2020, 29 (**4**): 048102. DOI: 10.1088/1674-1056/ab7807

Comparison study of GaN films grown on porous andplanar GaN templates

Shan Ding(丁姗), Yue-Wen Li(李悦文), Xiang-Qian Xiu(修向前), Xue-Mei Hua(华雪梅), Zi-Li Xie(谢自力), Tao Tao(陶涛), Peng Chen(陈鹏), Bin Liu(刘斌), Rong Zhang(张荣), You-Dou Zheng(郑有炓)
Chin. Phys. B, 2020, 29 (**3**): 038103. DOI: 10.1088/1674-1056/ab6c48

Coalbed methane adsorption and desorption characteristics related to coal particle size

Yan-Yan Feng(冯艳艳), Wen Yang (杨文), Wei Chu(储伟)
Chin. Phys. B, 2016, 25 (**6**): 068102. DOI: 10.1088/1674-1056/25/6/068102

Adsorption of CO_2 on MgAl layered double hydroxides: Effect of intercalated anion and alkaline etching time*

Yan-Yan Feng(冯艳艳)[1,2], Xiao-Di Niu(牛潇迪)[1], Yong-Hui Xu (徐永辉)[1], and Wen Yang(杨文)[1,2,†]

[1] *Department of Chemistry and Bioengineering, Guilin University of Technology, Guilin* 541004, *China*
[2] *Guangxi Key Laboratory of Electrochemical and Magnetochemical Functional Materials, Department of Chemistry and Bioengineering, Guilin University of Technology, Guilin* 541004, *China*

(Received 25 September 2020; revised manuscript received 1 December 2020; accepted manuscript online 30 December 2020)

The adsorption of CO_2 on MgAl layered double hydroxides (MgAl-LDHs) based adsorbents has been an effective way to capture CO_2, however the adsorption capacity was hampered due to the pore structure and the dispersibility of adsorption active sites. To address the problem, we investigate the effect of intercalated anion and alkaline etching time on the structure, morphology and CO_2 uptake performances of MgAl-LDHs. MgAl-LDHs are synthesized by the one-pot hydrothermal method, followed by alkaline etching of NaOH, and characterized by x-ray diffraction, N_2 adsorption, scanning electron microscopy and Fourier transform infrared spectroscopy. The CO_2 adsorption tests of the samples are performed on a thermogravimetric analyzer, and the adsorption data are fitted by the first-order, pseudo-second-order and Elovich models, respectively. The results demonstrate that among the three intercalated samples, MgAl(Cl) using chloride salts as precursors possesses the highest adsorption capacity of CO_2, owing to high crystallinity and porous structure, while MgAl(Ac) employing acetate salts as precursors displays the lowest CO_2 uptake because of poor crystallinity, disorderly stacked structure and unsatisfactory pore structure. With regard to alkaline etching, the surface of the treated MgAl(Cl) is partly corroded, thus the specific surface area and pore volume increase, which is conducive to the exposure of adsorption active sites. Correspondingly, the adsorption performance of the alkaline-etched adsorbents is significantly improved, and MgAl(Cl)-6 has the highest CO_2 uptake. With the alkaline etching time further increasing, the CO_2 adsorption capacity of MgAl(Cl)-9 sharply decreases, mainly due to the collapse of pore structure and the fragmentized sheet-structure. Hence, the CO_2 adsorption performance is greatly influenced by alkaline etching time, and appropriate alkaline etching time can facilitate the contact between CO_2 molecules and the adsorbent.

Keywords: CO_2 adsorption, MgAl-LDHs, one-pot hydrothermal method, intercalated anion, alkaline etching

PACS: 81.05.Rm, 81.07.–b, 68.43.Mn **DOI:** 10.1088/1674-1056/abd750

1. Introduction

In recent years, with the fast speed of population growth and social development, human beings need more energy, along with the continuous progress of modernization and automation.[1] Up to date, most of the energy comes from fossil resources; however, the inadequate combustion of fossil resources and other irregular use of fossil resources not only wasted the earth's precious resources, but also produced a large number of toxic and harmful gases and fuel waste, resulting in serious environmental pollution.[2] The burning of fossil resources has produced a large amount of CO_2, which can cause obvious greenhouse effect and other serious environmental problems on earth.[3–5] This phenomenon has attracted worldwide attention, and in order to reduce CO_2 emission, the relevant factories have to install and design the process technology for CO_2 capture. Hence, it is necessary to strengthen the research on CO_2 adsorption.

There are many solid adsorbents to deal with CO_2, but more efficient methods with fast adsorption rate and low cost are needed. According to the adsorption temperature, CO_2 adsorbents can be divided into three types: low-temperature adsorbent (adsorption temperature below 200 °C),[6–8] medium-temperature adsorbent (adsorption temperature between 200 and 400 °C),[9] and high-temperature adsorbent (adsorption temperature above 400 °C).[10] For low-temperature adsorption, great efforts have been devoted to advancing the capture performance. Guo *et al.*[6] prepared a series of porous activated carbons derived from sugarcane bagasse, and compared with the physically activated carbons, the NaOH-activated carbon showed high dynamic CO_2 uptake of 1.31 mmol/g at 60 °C under 10% CO_2 flowing gas. Verrecchia *et al.*[7] investigated the three main factors affecting the synthesis of zeolites from coal fly ash, and then achieved the adsorbent with excellent CO_2 adsorption performance as compared to commercial 13X. Chen *et al.*[8] synthesized the premodified Li/Al hydrotalcite impregnated with polyethylenimine (PEI), and with PEI loading of 40%, the functionalized adsorbent obtained the highest adsorption capacity of 1.723 mmol/g at 50 °C.

Among abundant low-temperature solid adsorbents,

*Project supported by the National Natural Science Foundation of China (Grant No. 21606058), the Natural Science Foundation of Guangxi, China (Grant Nos. 2017GXNSFBA198193 and 2017GXNSFBA198124), and the Startup Foundation for Doctors of Guilin University of Technology (Grant No. GLUTQD2015008).

†Corresponding author. E-mail: yangwen167@163.com

© 2021 Chinese Physical Society and IOP Publishing Ltd

MgAl layered double hydroxides (MgAl-LDHs) have got a great deal of attention. LDHs, consisting of positively charged layers and interlayer anions, belong to anionic layered compounds. Owing to the mobility and strong interchangeability of interlayer anions,[11–13] LDHs have been applied in many fields, such as adsorption,[14–16] catalysis,[17–19] electrochemistry,[20,21] and flame retardant.[22,23] In terms of adsorption applications, MgAl-LDHs could not only remove CO_2 from industrial exhaust, but also collect the anionic pollutants in the environment and gas pollution, etc. To date, numerous research on MgAl-LDHs has focused on improving the preparation methods, including changing the molar ratio of Mg/Al,[24] modifying with alkali metals, replacing the intercalation anions,[25] and so on.[26,27] Among various preparation methods, the co-precipitation method is the most commonly used. However, for the obtained adsorbents, it is disadvantageous to CO_2 adsorption due to their small specific surface area and stacked structure. Therefore, it is of great significance to promote the CO_2 uptake of MgAl-LDHs with loose and porous structure.

In the present study, MgAl-LDHs are obtained via the one-pot hydrothermal method. Due to the amphoteric nature of Al species, NaOH is used to remove the Al species in the LDHs,[28] and appropriate treating time with NaOH solution would contribute meaningfully to forming some nanopores and increasing the available specific surface area, which ultimately expose more effective adsorption sites for CO_2 uptake. Consequently, we investigate the effect of intercalated anion and alkaline etching time on the structure and morphology of MgAl-LDHs for use in CO_2 uptake. Adjusting the intercalated anion and alkaline etching time of LDHs can tailor the structural characteristics of the resultant adsorbents, which in turn tune their adsorption performances, for MgAl-LDHs with high specific surface area and large pore volume are beneficial to the CO_2 adsorption process. After that, the adsorbents are characterized by x-ray diffraction (XRD), N_2 adsorption, scanning electron microscopy (SEM) and Fourier transform infrared spectroscopy (FT-IR), respectively, followed by adsorption measurement of CO_2. In order to explore the adsorption mechanism, the adsorption data are fitted by the first-order, pseudo-second-order and Elovich models, respectively. In general, this work would provide meaningful guidance for designing MgAl-LDHs to improve CO_2 adsorption performance.

2. Experimental details

2.1. Materials

In experiment, magnesium nitrate hexahydrate (99.0%, $Mg(NO_3)_2{\cdot}6H_2O$), aluminum nitrate nonahydrate (99.0%, $Al(NO_3)_3{\cdot}9H_2O$), magnesium chloride hexahydrate (98.0%, $MgCl_2{\cdot}6H_2O$), aluminum chloride hexahydrate (97.0%, $AlCl_3{\cdot}6H_2O$), magnesium acetate tetrahydrate (99.0%, $Mg(CH_3COO)_2{\cdot}4H_2O$), aluminum acetate ($Al(CH_3COO)_3$), urea (99.0%, H_2NCONH_2), and sodium hydroxide (96.0%, NaOH) were analytical grade and purchased from Xilong Chemical Co. Ltd., Guangzhou, China. All the chemicals were used without further purification.

2.2. Preparation of the samples

2.2.1. Preparation of MgAl-LDHs intercalated with different anions

The MgAl-LDH adsorbents intercalated with different anions (NO_3^-, Cl^-, Ac^-) were synthesized by the one-pot hydrothermal method,[12,29,30] and the molar ratio of Mg/Al was 2 : 1. Taking MgAl-LDHs intercalated with NO_3^- anion as an example, 0.01 mol of $Mg(NO_3)_2{\cdot}6H_2O$ and 0.005 mol of $Al(NO_3)_3{\cdot}9H_2O$ were added to 40 mL of deionized water, followed by stirring at room temperature. Once the precursor was dissolved, 0.075 mol of urea was added into the metal nitrate salt solution, and the mixture was kept under stirring until the added urea was completely dissolved. Subsequently, the solution was transferred to autoclaves at 120 °C for 12 h. After cooling to room temperature, the as-prepared product was washed with water and ethanol for several times. Finally, the resulting powders were dried at 100 °C overnight and labeled as MgAl(NO). In addition, the samples MgAl(Cl) and MgAl(Ac) were also obtained with the same preparation method, where Cl and Ac represented the metal chloride salts and acetate salts used, respectively.

2.2.2. Preparation of the adsorbents alkaline-etched by 3.0 mol/L NaOH

The adsorbents alkaline-etched by 3.0 mol/L NaOH were prepared as follows.[28] A 50 mL NaOH solution with 0.2 g of MgAl(Cl) was fully stirred at room temperature for 30 min, followed by alkaline etching reaction at 95 °C for 3, 6 and 9 h, respectively. Finally, the product was washed with water and ethanol for several times and dried at 100 °C overnight, named as MgAl(Cl)-3, MgAl(Cl)-6, and MgAl(Cl)-9, respectively.

2.3. Characterization

XRD patterns of the samples were characterized by a power x-ray diffractometer (PANalytical X'Pert3) with Cu K_α radiation.[21] The pore structure of the samples was obtained using N_2 physisorption at 77 K by a Micromeritics ASAP Tristar Ⅱ 3020 equipment (Micromeritics Instrument Corporation). Prior to the analysis, the sample was degassed at 150 °C for 3 h. The morphology of the samples was observed using a field-emission scanning electron microscope (SEM, Hitachi SU5000). FT-IR spectra were conducted on a Fourier transform infrared spectrometer (Nicolet iS10, Amer-

ican Thermo Scientific Company) in the wavelength range of 400–4000 cm^{-1}.

2.4. CO_2 adsorption capacity evaluation

The CO_2 adsorption performance of the samples was tested by a thermogravimetric analyzer (SDT Q500, TA).[31] Appropriately 10 mg of the sample was put into an alumina pan, and He was injected as a protective gas with a gas flow of 100 mL/min. Next, the sample was raised to 75 °C with a heating rate of 5 °C/min. After stabilizing at 75 °C for 30 min, the gas was switched to CO_2 with a gas flow of 100 mL/min, and the adsorption process was kept at 75 °C for 60 min. The adsorption amount of CO_2 was calculated according to the weight change of the sample during the adsorption process.

The first-order (Eq. (1)),[32] the pseudo-second-order (Eq. (2)),[33] and Elovich (Eq. (3))[34] kinetic models are applied over the as-prepared adsorbents, and the kinetic models are expressed as follows:

$$\log(q_{e,1} - q_t) = \log q_{e,1} - \left(\frac{k_1}{2.303}\right)t, \tag{1}$$

$$\frac{t}{q_t} = \frac{1}{k_2 q_{e,2}^2} + \left(\frac{1}{q_{e,2}}\right)t, \tag{2}$$

$$q_t = \left(\frac{1}{\beta}\right)\ln(k\beta) + \left(\frac{1}{\beta}\right)\ln t, \tag{3}$$

where $q_{e,1}$ ($q_{e,2}$) is the adsorption capacity of MgAl-LDHs at equilibrium (mg/g); q_t is the adsorption capacity (mg/g) of CO_2 by the adsorbent at time t (min); k_1 (1/min), k_2 (g/(mg·min)) and k are the first-order, pseudo-second-order and Elovich rate constants, respectively; β is the relationship between surface coverage and activation energy.

3. Results and discussion

3.1. Characterization analyses

The XRD patterns of the samples are presented in Fig. 1. Characteristic diffraction features of the LDHs structure appear in all MgAl-LDHs samples at 2θ of 11.5°, 23.6°, 35.0°, 39.6° and 47.1°, corresponding to the reflections of (003), (006), (009), (015), and (018), respectively.[35] The sample MgAl(Cl) synthesized with chloride salts as precursors shows higher crystallinity than the samples MgAl(NO) and MgAl(Ac), suggesting that the crystallinity is affected by the precursor nature. In addition, the characteristic peaks of $Mg_5(CO_3)_4(OH)_2{\cdot}4H_2O$ (brucite) are observed for MgAl(Ac) using acetate salts as precursors. As for the alkaline-etched adsorbents shown in Fig. 1(b), the characteristic peak of LDHs also appears, and the characteristic peaks at 2θ of 23.6° and 47.1° change from single peak to double peaks. As the samples undergo alkaline etching, the characteristic peaks of $Mg_6Al_2(OH)_{18}{\cdot}4.5H_2O$ would obviously appear, while the characteristic peaks of $Mg_4Al_2(OH)_{14}{\cdot}3H_2O$ decrease, revealing that the Al species are partly removed. With the further increase of the alkaline etching time, the characteristic peaks of $Mg_4Al_2(OH)_{14}{\cdot}3H_2O$ are gradually weakened.

N_2 adsorption isotherms of the samples are depicted in Fig. 2. All the samples exhibit typical type-Ⅲ isotherms with low N_2 uptake at low relative pressure (P/P_0) and high N_2 uptake at high P/P_0. For MgAl-LDHs intercalated with different anions, the adsorption volume of MgAl(Cl) is highest among the three samples, while the adsorption volume of MgAl(Ac) is lowest. With the alkaline etching of NaOH, the N_2 adsorption capacity depicts a reverse U-shaped trend. As the alkaline etching time increases, the N_2 uptake of MgAl(Cl)-3 gradually increases, and the adsorption capacity of MgAl(Cl)-6 reaches the maximum. With further increase of the alkaline etching time, the adsorption capacity of MgAl(Cl)-9 obviously decreases. The above results indicate that the alkaline etching time has a significant influence on the pore structure of the MgAl-LDHs.

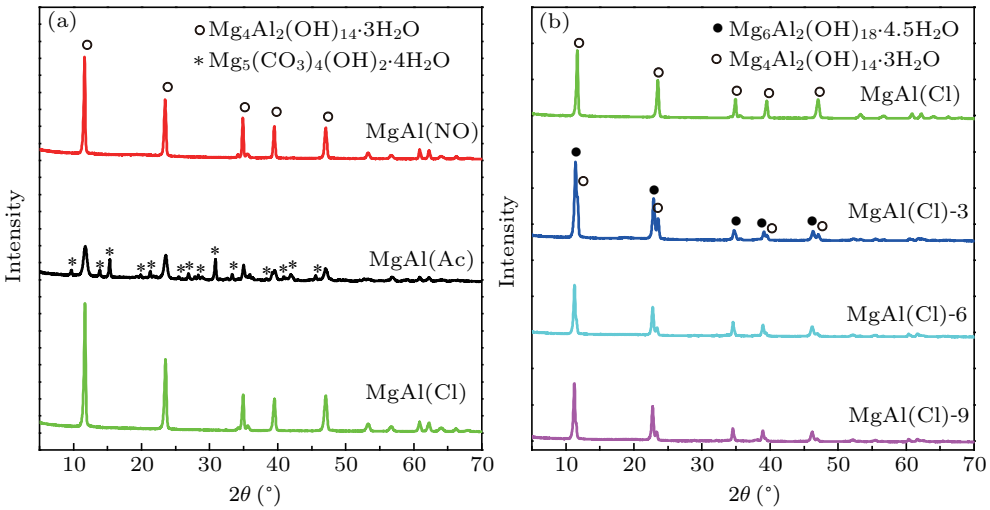


Fig. 1. XRD patterns of the samples.

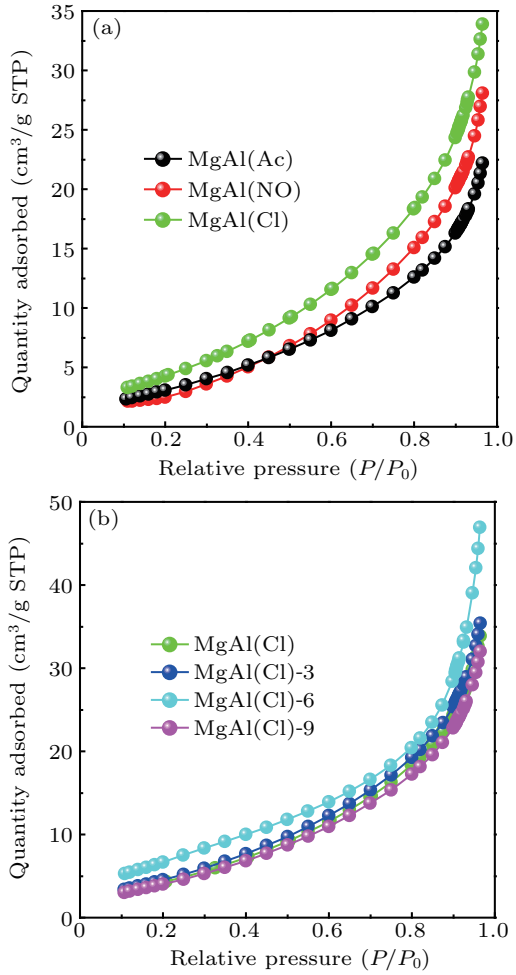


Fig. 2. N_2 adsorption isotherms of the samples.

Figure 3 displays pore size distributions (PSD) of the samples computed with the Barrett–Joyner–Halenda (BJH) method. As shown in Fig. 3, all the samples possess a distribution of pores within the diameters of 0–50 nm, confirming the formation of mesoporous materials, which is attributed to the stacked structure of LDHs. It is noted that the mesopore volume of MgAl(Cl) within 2–50 nm is higher than that of MgAl(Ac) and MgAl(NO), in good agreement with the N_2 adsorption isotherms, and is further expanded after alkaline etching treatment. With the alkaline etching time of 9 h, the pores of MgAl(Cl)-9 collapse and the corresponding mesopore volume declines. For the alkaline-etched adsorbents, MgAl(Cl)-6 possesses huge number of micropores and mesopores, revealing that alkaline etching could make the significant contribution of micropores and mesopores, especially mesopores. This also explains why the sample MgAl(Cl)-6 achieves an enhanced CO_2 adsorption capacity.

Figure 4 presents the Brunauer–Emmett–Teller specific surface area (BET SSA) and pore volume (PV) of the samples. The variation of intercalated anions leads to differences in the BET SSA and PV. Among the intercalated adsorbents, the MgAl(Cl) using chloride salts as precursors displays the highest BET SSA and PV, indicating that the porosity of MgAl(Cl) is well-developed. Compared with others, the MgAl(NO) sample has the lowest BET SSA, being 86.5% and 66.0% of the MgAl(Ac) and MgAl(Cl), respectively. The alkaline etching of NaOH results in high surface areas and large pore volumes, and the MgAl(Cl)-6 sample achieves the largest BET SSA of 28.13 m^2/g and PV of 0.0765 cm^3/g.

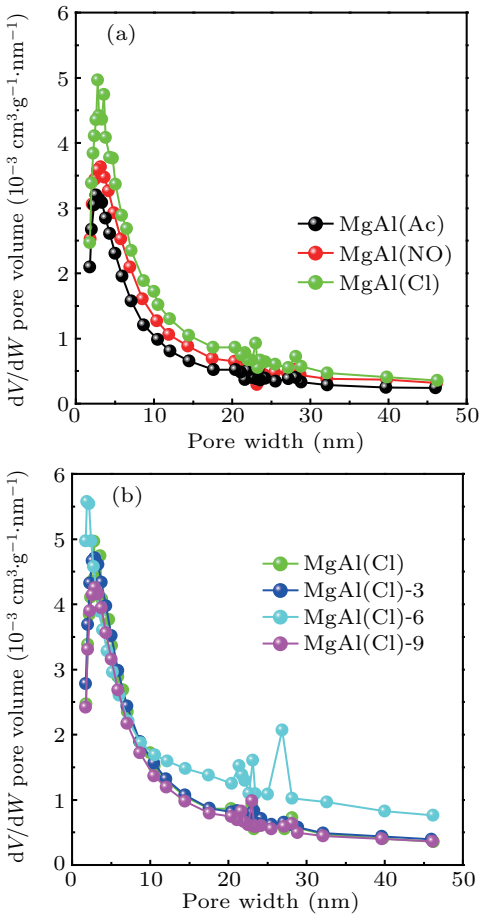


Fig. 3. Pore size distributions of the samples obtained by the BJH adsorption branch.

SEM characterization results of the samples are shown in Fig. 5. Sheet-like LDHs with smooth surface of MgAl(NO) and MgAl(Cl) using chloride salts and nitrate salts as precursors can be observed in Figs. 5(a) and 5(c), while disorderly stacked structure of MgAl(Ac) with acetate salts as precursors can be seen from Fig. 5(b). The different morphologies presented by the MgAl-LDHs with different precursors may be due to the nature of intercalated anions. After alkaline etching treatment, the layered structure begins to be destroyed, suggesting that the Al species of the layered structure are partly removed, along with the increase of BET SSA and PV of the modified LDHs, which would be conducive to the exposure of the active sites, so as to improve the adsorption performance of the adsorbent. Nevertheless, the longer the alkaline etching time, the more serious the structural damage, and with the alkaline etching time being 9 h, the sheet-like structure of MgAl(Cl)-9 is severely crushed and aggregated, resulting

in poor dispersibility, which is consistent with the results of N_2 adsorption analysis.

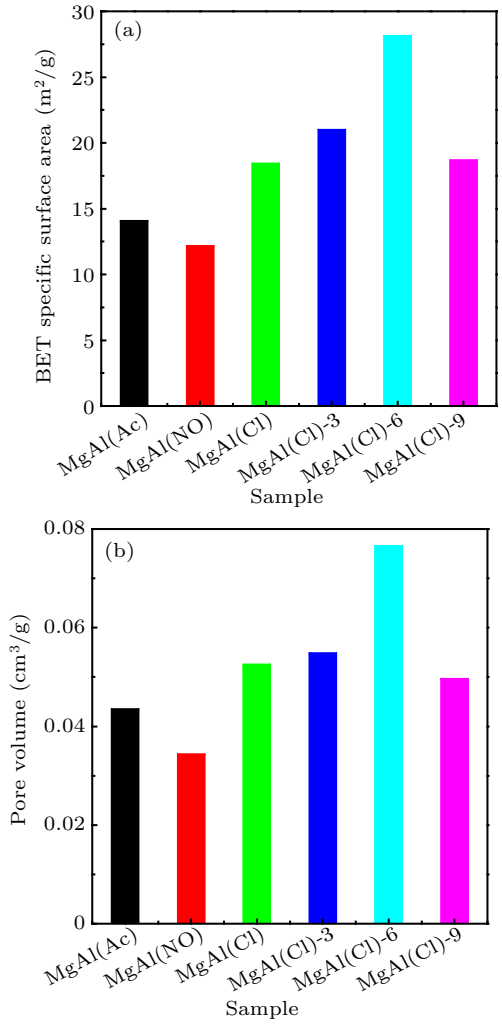


Fig. 4. BET specific surface area (a) and pore volume (b) of the samples.

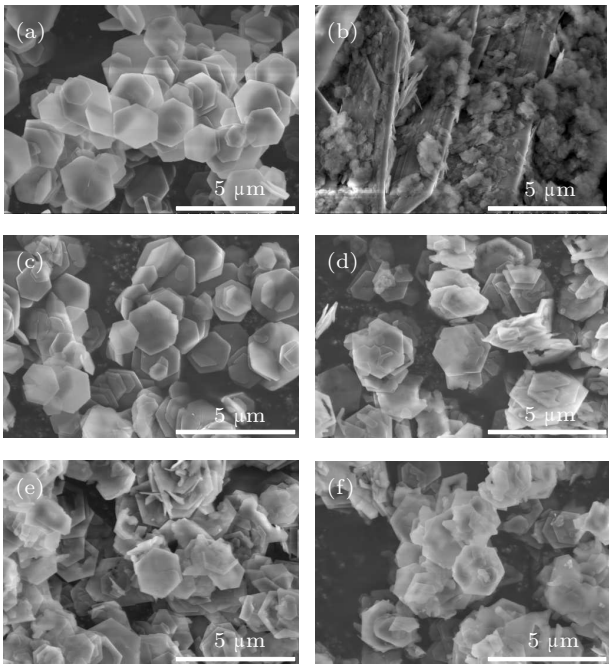


Fig. 5. SEM images of the samples: (a) MgAl(NO), (b) MgAl(Ac), (c) MgAl(Cl), (d) MgAl(Cl)-3, (e) MgAl(Cl)-6, and (f) MgAl(Cl)-9.

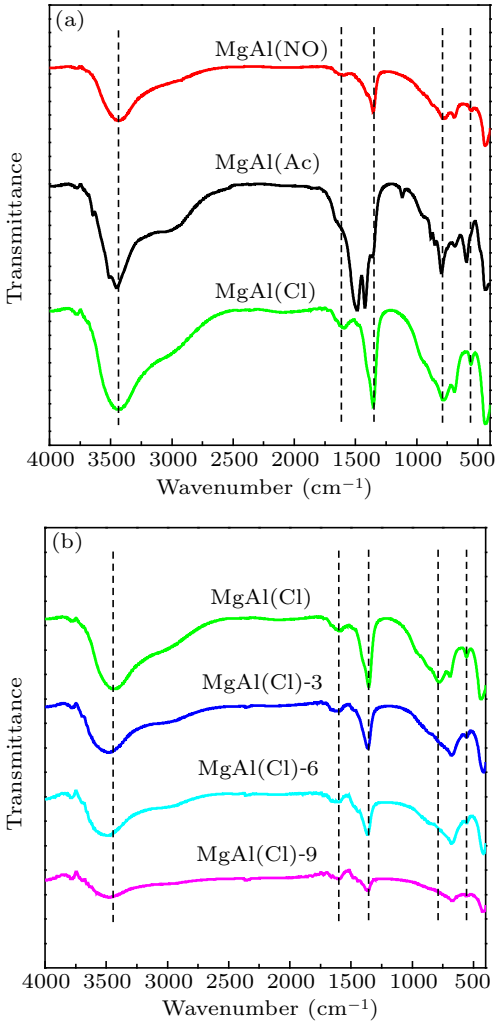


Fig. 6. FT-IR spectra of the samples.

In order to explore the interlayer groups, FT-IR analysis was performed for the samples, and the results are exhibited in Fig. 6. The intense band around 3400 cm^{-1} is assigned to the OH stretching vibration of interlayer water and hydrogen bond,[36] while the weak band in 1650 cm^{-1} corresponds to the bending vibration of water molecules presented in the samples.[37] With using the urea as precipitant, the absorption peak of NH_4^+ in 1362 cm^{-1} is observed. For the sample MgAl(Ac), a signal appeared at 1380 cm^{-1} is assigned to characteristic peaks of symmetric stretching vibration of C–O bond in carboxylate (COO^-). The characteristic vibration peaks of Mg and Al species are in the range of 400–800 cm^{-1}.[38] Bands around 780 cm^{-1} and 550 cm^{-1} are assigned to characteristic peaks of Al–OH and Mg–OH, respectively; the intensity of these bands is higher in the sample MgAl(Cl), demonstrating its higher crystallinity, in agreement with the XRD results. Moreover, with alkaline etching, a decrease in the signal related with vibration of Al–OH is noticed.

3.2. CO_2 adsorption performances of the adsorbents

The effect of intercalated anion and alkaline etching time on CO_2 adsorption for MgAl-LDH adsorbents was performed,

and in order to analyze the adsorption mechanism of CO_2 on the adsorbent, the adsorption data are fitted by the first-order kinetic equation, the pseudo-second-order kinetic equation and the Elovich model, respectively. Figure 7(a) exhibits the CO_2 adsorption data of the MgAl-LDHs with different precursors. Obviously, the intercalated anion could influence CO_2 adsorption behavior, and it is meaningful to apply the suitable precursor to prompt CO_2 adsorption performance of MgAl-LDHs. Among the three samples, the adsorbent MgAl(Cl) possesses the highest CO_2 adsorption capacity. The impact of intercalated anion for MgAl-LDHs on CO_2 adsorption behavior and adsorption kinetics is illustrated in Figs. 7(b)–7(d) and Table 1. Compared with the first-order kinetic equation and the Elovich model, the correlation coefficient R^2 for the pseudo-second-order kinetic equation is close to 1.0, suggesting that the fitting curves are in good agreement with the adsorption data and the adsorption process is more suitable to be described by the pseudo-second-order kinetic equation.

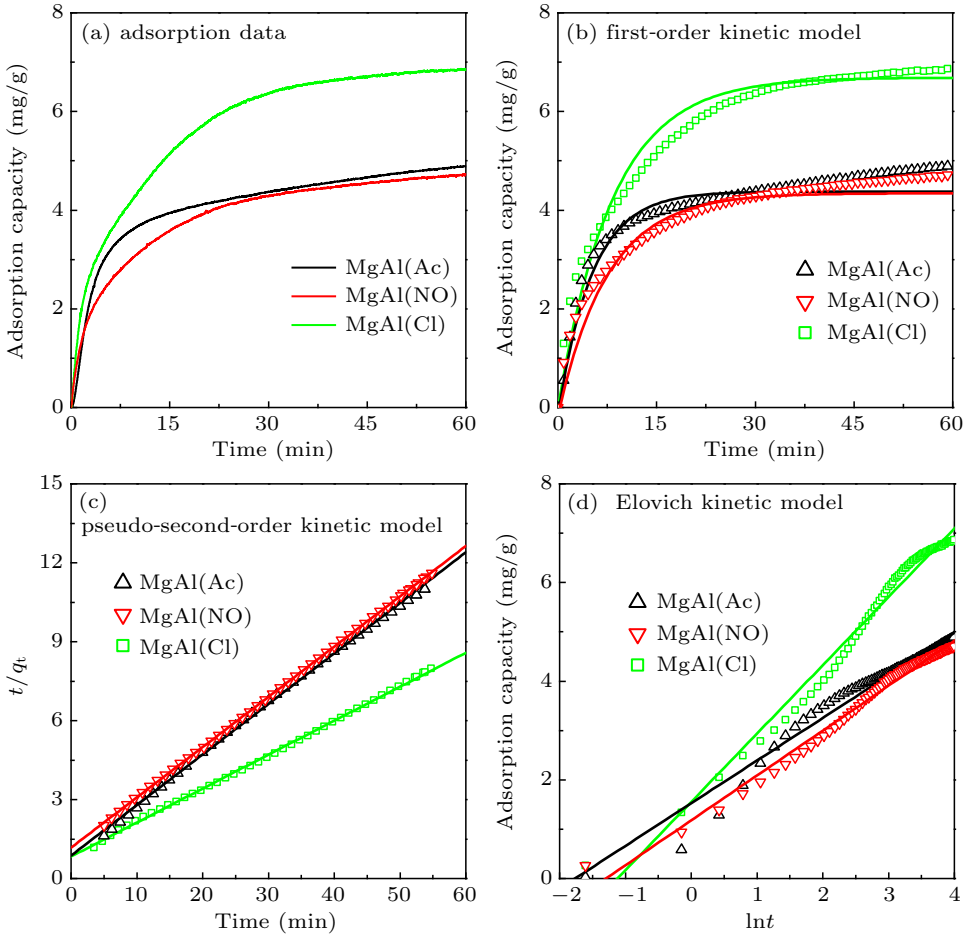


Fig. 7. CO_2 adsorption isotherms of the samples prepared with different precursors fitted by the first-order kinetic model, the pseudo-second-order kinetic model, and the Elovich kinetic model.

In the initial stage of adsorption, the adsorption rate of the samples is faster; however, as the adsorption process progresses, the adsorption rate slows down and the adsorption equilibrium would be reached after a period of time. It is found that the CO_2 adsorption process of the samples could be divided into two stages: rapid surface reaction stage and CO_2 diffusion controlling stage. In the rapid surface reaction stage, the large slope of the curve indicates the fast adsorption rate. Among the intercalated samples, the adsorption rate of MgAl(Ac) is higher, and thus its CO_2 adsorption capacity hardly changes after 15 min. The rapid reaction stage is the important stage of adsorption, that is, CO_2 reacts with the alkaline binding sites on the adsorbent surface; with the progress of adsorption, the adsorption site of the adsorbent is gradually covered, which slows down the adsorption rate. As the adsorption process of CO_2 for MgAl(NO) and MgAl(Ac) reaches saturation, the adsorption capacity of MgAl(Cl) still increases, ascribing to the developed pore structure and abundant alkaline adsorption sites. In addition, it should be noted that the crystallinity of MgAl-LDHs has a non-negligible effect on CO_2 adsorption performance, and high crystallinity leads to favorable CO_2 uptake.

Figure 8 shows CO_2 uptake of alkaline-etched MgAl(Cl) adsorbents. It can be seen that the adsorption performance of the adsorbents is significantly improved after alkaline etching, and the sample MgAl(Cl)-6 with alkaline etching time of 6 h has the highest adsorption amount of 16.3 mg/g. As the alkaline etching time continues to extend, the CO_2 up-

take of MgAl(Cl)-9 sharply decreases, due to the collapse of pore structure and the fragmentized sheet-structure. Hence, the CO_2 adsorption performance is greatly influenced by alkaline etching time, and appropriate alkaline etching time can advance the contact between CO_2 molecules and the adsorbent. The fitting results of the kinetic models (displayed in Figs. 8(b)–8(d) and Table 1) show that both the first-order and pseudo-second-order kinetic models are applicable, and thus the adsorption process includes physical adsorption and chemical adsorption; however, the correlation coefficients of the pseudo-second-order kinetic model are slightly higher than those of the first-order kinetic model, indicating that the adsorption process of the adsorbent on CO_2 is more obedient to the pseudo-second-order kinetic model than to the first-order kinetic model. The sample MgAl(Cl)-6 owns the fastest adsorption rate of 0.041 g/(mg·min), while MgAl(Cl) without alkaline etching has the lowest adsorption rate of 0.020 g/(mg·min), consistent with CO_2 adsorption capacities of the alkaline-etched samples, which indicates that alkaline etching treatment is conducive to the internal diffusion of CO_2 during the adsorption process.

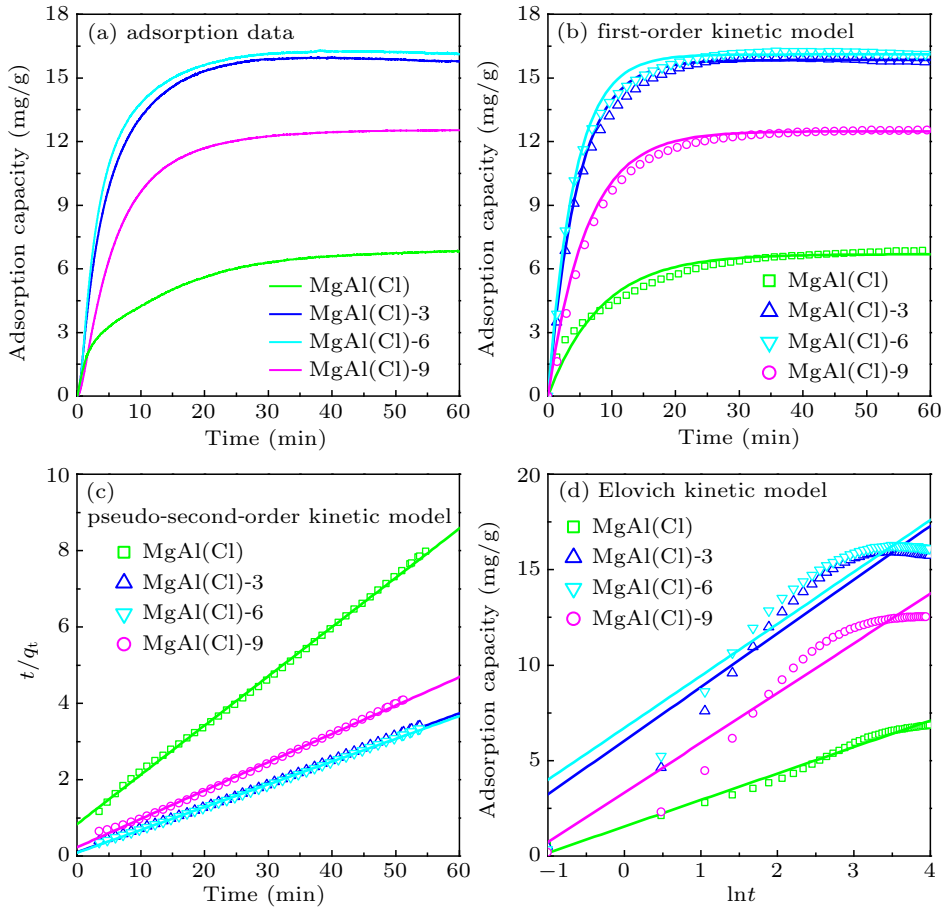


Fig. 8. CO_2 adsorption isotherms of the samples prepared with various alkaline etching times fitted by the first-order kinetic model, the pseudo-second-order kinetic model, and the Elovich kinetic model.

Table 1. Adsorption parameters from kinetic models of CO_2 adsorption data.

Sample	First-order kinetic model			Pseudo-second-order kinetic model			Elovich model		
	R^2	$q_{e,1}$	k_1	R^2	$q_{e,2}$	k_2	R^2	β	k
MgAl(Ac)	0.939	4.54	0.193	0.998	5.21	0.042	0.961	1.157	5.054
MgAl(NO)	0.958	4.51	0.132	0.999	5.24	0.031	0.981	1.099	3.324
MgAl(Cl)	0.966	6.69	0.120	0.999	7.75	0.020	0.972	0.722	4.245
MgAl(Cl)-3	0.997	15.84	0.212	0.999	16.49	0.037	0.867	0.356	24.089
MgAl(Cl)-6	0.993	16.11	0.240	0.999	16.76	0.041	0.857	0.368	32.121
MgAl(Cl)-9	0.997	12.48	0.164	0.999	13.47	0.024	0.906	0.384	9.334

4. Conclusions

MgAl layered double hydroxides have been synthesized by the one-pot hydrothermal method to investigate the effect of intercalated anion and alkaline etching time on CO_2 adsorption. By means of XRD, N_2 adsorption, SEM, FT-IR and CO_2 adsorption analyses, the results demonstrate that the adsorbent MgAl(Cl) using chloride salts as precursors shows a high crys-

tallinity, sheet-like LDHs with smooth surface and developed pore structures. In contrast, MgAl(Ac) employing acetate salts as precursors displays a poor crystallinity, disorderly stacked structure and unsatisfactory pore structure; and correspondingly, MgAl(Cl) possesses the highest CO_2 uptake among the three intercalated samples. With alkaline etching of NaOH, the adsorption performance of the adsorbents is significantly improved, and MgAl(Cl)-6 with alkaline etching time of 6 h has the largest adsorption amount of 16.3 mg/g, which could be ascribed to well-developed porosity. The alkaline adsorption active sites over the surface of the adsorbent are fully exposed, which is conducive to the combination of acid gas CO_2 with it, thereby enhancing the CO_2 capture. As the alkaline etching time further increases, the CO_2 adsorption capacity of MgAl(Cl)-9 obviously reduces, mainly due to the collapse of pore structure and the fragmentized sheet-structure. Therefore, this work would provide a valuable idea for the rational design of MgAl-LDHs for enhancing CO_2 adsorption.

References

[1] Yang W, Feng Y Y, Xiao D and Yuan H Y 2015 *Int. J. Energ. Res.* **39** 805

[2] Shahkarami S, Dalai A K and Soltan J 2016 *Ind. Eng. Chem. Res.* **55** 5955

[3] Kwon H J, Kwon S, Seo J G, Jung I S, Son Y H, Lee C H, Lee K B and Lee H C 2017 *ChemSusChem* **10** 1701

[4] Feng Y Y, Yang W, Chen S and Chu W 2014 *Integr. Ferroelectr.* **151** 116

[5] Yao L H, Cao M S, Yang H J, Liu X J, Fang X Y and Yuan J 2014 *Comput. Mater. Sci.* **85** 179

[6] Guo Y F, Tan C, Sun J, Li W L, Zhang J B and Zhao C W 2020 *Chem. Eng. J.* **381** 122736

[7] Verrecchia G, Cafiero L, Caprariis B D, Dell'Era A, Pettiti I, Tuffi R and Scarsella M 2020 *Fuel* **276** 118041

[8] Chen S P, Sun X Y, Luo X and Liang Z W 2019 *Ind. Eng. Chem. Res.* **58** 1177

[9] Wang K, Zhao Y W, Clough P T, Zhao P F and Anthony E J 2019 *Chem. Eng. J.* **372** 886

[10] Guo H X, Xu Z H, Tao J, Zhao Y J, Ma X B and Wang S P 2020 *J. CO_2 Util.* **37** 335

[11] Wang J, Wei Y and Yu J 2013 *Appl. Clay Sci.* **72** 37

[12] Jamil S, Khan S R, Alvi A R, Kausar F, Ali S, Khan S A, Naim M, Malik A and Janjua M R 2020 *Chem. Phys.* **528** 110530

[13] Zhou Y, Liu Z, Bo A, Tana T, Liu X, Zhao F, Sarina S, Jia M, Yang C and Gu Y 2020 *J. Hazard. Mater.* **382** 121111

[14] Kou X, Guo H, Ayele E G, Li S, Zhao Y, Wang S and Ma X 2018 *Energ. Fuel.* **32** 5313

[15] Xu Z X, Song H, Li P J, Zhu X and Hu X 2020 *J. Hazard. Mater.* **398** 122833

[16] Kong X, Chen J, Tang Y, Lv Y and Wang H 2020 *J. Hazard. Mater.* **392** 122392

[17] Ma Q, Nengzi L, Li B, Wang Z, Liu L and Cheng X 2020 *Sep. Purif. Technol.* **235** 116204

[18] Lestari P R, Takei T, Yanagida S and Kumada N 2020 *Mater. Chem. Phys.* **250** 122988

[19] Tao X, Yang C, Huang L and Xu D 2020 *Mater. Chem. Phys.* **250** 123118

[20] Zhang D, Guo X, Tong X, Chen Y and Zhang J 2020 *J. Alloy. Compd.* **837** 155529

[21] Feng Y Y, Li Y J, Yang W and Huang H B 2020 *J. Nanosci. Nanotechnol.* **20** 1260

[22] Hajibeygi M, Mousavi M, Shabanian M and Vahabi H 2020 *Mater. Today Commun.* **23** 100880

[23] Xu S, Zhang M, Li S Y, Zeng H Y and Pan Y 2020 *Appl. Clay Sci.* **191** 105600

[24] Sharma U, Tyagi B and Jasra R V 2008 *Ind. Eng. Chem. Res.* **47** 9588

[25] Wang Q, Wu Z, Tay H H, Chen L, Liu Y, Chang J, Zhong Z, Luo J and Borgna A 2011 *Catal. Today* **164** 198

[26] Hu G, Wang N, Ohare D and Davis J J 2006 *Chem. Commun.* **3** 287

[27] Paredes S P, Fetter G, Bosch P and Bulbulian S 2006 *J. Mater. Sci.* **41** 3377

[28] Lu Z Y, Zhu W, Lei X D, Williams G R, O'Hare D, Chang Z, Sun X M and Duan X 2012 *Nanoscale* **4** 3640

[29] Wu P, Xia L, Liu Y, Wu J, Chen Q and Song S 2018 *ACS Sustain. Chem. Eng.* **6** 16287

[30] Naseem S, Gevers B, Boldt R, Labuschagné F G W and Leuteritz A 2019 *RSC Adv.* **9** 3030

[31] Peng J, Iruretagoyena D and Chadwick D 2018 *J. CO_2 Util.* **24** 73

[32] Zhang H, Hu J, Xie J, Wang S and Cao Y 2019 *RSC Adv.* **9** 2011

[33] Tuerk T, Alp I and Deveci H 2009 *J. Hazard. Mater.* **171** 665

[34] Zhu X, Shi Y and Cai N 2017 *Fuel* **207** 579

[35] Borges G A, Ferreira G M D, Siqueira K P F, Dias A and Mageste A B 2020 *J. Colloid Interf. Sci.* **575** 194

[36] Cocheci L, Lupa L, Tolea N S, Muntean C and Negrea P 2020 *Sep. Purif. Technol.* **250** 117104

[37] Thouchprasitchai N, Pintuyothin N and Pongstabodee S 2017 *J. Environ. Sci.* **65** 293

[38] Othman M R, Rasid N M and Fernando W J N 2006 *Chem. Eng. Sci.* **61** 1555